

# Decorin Protein Core Affects the Global Gene Expression Profile of the Tumor Microenvironment in a Triple-Negative Orthotopic Breast Carcinoma Xenograft Model

Simone Buraschi<sup>1,3</sup>, Thomas Neill<sup>1,3</sup>, Rick T. Owens<sup>2</sup>, Leonardo A. Iniguez<sup>3</sup>, George Purkins<sup>1</sup>, Rajanikanth Vadigepalli<sup>1</sup>, Barry Evans<sup>1</sup>, Liliana Schaefer<sup>4</sup>, Stephen C. Peiper<sup>1</sup>, Zi-Xuan Wang<sup>1</sup>, Renato V. Iozzo<sup>1\*</sup>

**1** Department of Pathology, Anatomy and Cell Biology, and the Cancer Cell Biology and Signaling Program, Kimmel Cancer Center, Thomas Jefferson University, Philadelphia, Pennsylvania, United States of America, **2** LifeCell Corporation, Branchburg, New Jersey, United States of America, **3** Roche NimbleGen, Inc., Research and Development, Madison, Wisconsin, United States of America, **4** Department of Pharmacology, Goethe University, Frankfurt, Germany

## Abstract

Decorin, a member of the small leucine-rich proteoglycan gene family, exists and functions wholly within the tumor microenvironment to suppress tumorigenesis by directly targeting and antagonizing multiple receptor tyrosine kinases, such as the EGFR and Met. This leads to potent and sustained signal attenuation, growth arrest, and angiostasis. We thus sought to evaluate the tumoricidal benefits of systemic decorin on a triple-negative orthotopic breast carcinoma xenograft model. To this end, we employed a novel high-density mixed expression array capable of differentiating and simultaneously measuring gene signatures of both *Mus musculus* (stromal) and *Homo sapiens* (epithelial) tissue origins. We found that decorin protein core modulated the differential expression of 374 genes within the stromal compartment of the tumor xenograft. Further, our top gene ontology classes strongly suggests an unexpected and preferential role for decorin protein core to inhibit genes necessary for immunomodulatory responses while simultaneously inducing expression of those possessing cellular adhesion and tumor suppressive gene properties. Rigorous verification of the top scoring candidates led to the discovery of three genes heretofore unlinked to malignant breast cancer that were reproducibly found to be induced in several models of tumor stroma. Collectively, our data provide highly novel and unexpected stromal gene signatures as a direct function of systemic administration of decorin protein core and reveals a fundamental basis of action for decorin to modulate the tumor stroma as a biological mechanism for the ascribed anti-tumorigenic properties.

**Citation:** Buraschi S, Neill T, Owens RT, Iniguez LA, Purkins G, et al. (2012) Decorin Protein Core Affects the Global Gene Expression Profile of the Tumor Microenvironment in a Triple-Negative Orthotopic Breast Carcinoma Xenograft Model. PLoS ONE 7(9): e45559. doi:10.1371/journal.pone.0045559

**Editor:** Joseph J. Barchi, National Cancer Institute at Frederick, United States of America

**Received:** May 14, 2012; **Accepted:** August 21, 2012; **Published:** September 19, 2012

**Copyright:** © 2012 Buraschi et al. This is an open-access article distributed under the terms of the Creative Commons Attribution License, which permits unrestricted use, distribution, and reproduction in any medium, provided the original author and source are credited.

**Funding:** This work was in part supported by the National Institutes of Health grants RO1 CA39481, RO1 CA47282 and RO1 CA120975 (to RVI), and training grant T32 AA07463 (to TN). The funders had no role in study design, data collection and analysis, decision to publish, or preparation of the manuscript. No additional external funding received for this study.

**Competing Interests:** RTO works for LifeCell Co. and has provided the recombinant decorin used for the studies. LAI works for Roche-NimbleGen Co. and has provided expertise in performing the microarray data. There are no patents, products in development or marketed products to declare. This does not alter the authors' adherence to all the PLOS ONE policies on sharing data and materials.

\* E-mail: iozzo@kimmelcancercenter.org

These authors contributed equally to this work.

## Introduction

The traditional view of tumorigenesis has long been considered in the perspective of oncogenes and tumor suppressor genes governing diverse cellular processes such as cell proliferation, survival, migration, and metastasis, with a prominent focus on understanding the cellular imbalance existing among these two populations of nuclear encoded genes. However, the importance of the surrounding tumor environment has begun to emerge as an active participant in orchestrating many aspects of tumor growth and progression including invasion, metastasis, and angiogenesis [1,2]. The heterogeneous interactions between neoplastic cells and stromal components such as fibroblasts, tumor macrophages, extracellular matrix, host and tumor endothelial cells as well as basement membrane, collectively known as the tumor microenvironment, can have profound effects on tumorigenesis. However, despite the importance of tumor-stroma interactions, there is a

limited understanding of its composition and how the complex inter-relationships between growing malignant cells and stromal constituents take place.

The stromal-specific decorin is encoded by a large and complex gene (*DCN*) located on chromosome 12q23 which contains two alternatively-spliced leader exons [3] and a quite complex promoter region [4,5]. Notably, *DCN* transcriptional activity is induced by hypomethylation of its promoter [6,7] and by quiescence [8,9], and inhibited by TNF $\alpha$  [9], TGF $\beta$  [10] and viral oncogenes [11]. Decorin is a secreted small leucine-rich proteoglycan that binds collagen I and regulates fibrillogenesis [12–23], and is known to bind avidly to TGF $\beta$  [24] and regulate its bioactivity [25–27]. In addition, decorin-deficient mice are less susceptible to experimental infection by *Borrelia burgdorferi*, the spirochete responsible for Lyme disease in humans [28,29].

When in soluble form, decorin inhibits tumor growth by downregulating several receptor tyrosine kinases (RTKs) [30] such as the EGFR [31–34], IGF-IR [35–38], and Met [39–41] primarily by evoking caveolin-mediated internalization and degradation [31,39,42]. This leads to mobilization of intracellular calcium [43], concurrent induction of cyclin-dependent kinase inhibitor p21<sup>WAF1</sup> [44,45] and subsequent degradation of key downstream effectors such as  $\beta$ -catenin and Myc in various tumor xenografts [40].

Under growth conditions,  $\beta$ -catenin and Myc are stabilized by activation of Wnt and various RTK signaling pathways, which are often hyperactive in cancer. Thus, upstream activation of these signaling pathways leads to inactivating phosphorylation of GSK-3 $\beta$  by PI3K/Akt to allow for translocation of active  $\beta$ -catenin and Myc into the nucleus where, through association with various nuclear co-activator complexes, enable induction of a large number of genes including Myc itself [46,47], and AP4, a transcriptional repressor of p21 [48]. In contrast, decorin, by neutralizing the activity of EGFR and Met, relieves GSK3 $\beta$  inactivation, and leads to non-canonical GSK3 $\beta$ -evoked phosphorylation of  $\beta$ -catenin as well as Myc at Thr58 [39,40], thus leading to 26S proteasomal degradation. Thereby, the synthesis of AP4 would cease and p21 would be released from Myc/AP4-mediated transcriptional repression, as a direct biological manifestation of decorin-evoked suppression of RTK activity and tumorigenic growth [49]. Moreover, the relevance of decorin in cancer progression has been demonstrated in mutant mice where  $\sim$ 30% of decorin-null mice develop spontaneous intestinal tumors [50], whereas decorin-null mice carrying a targeted disruption in p53 succumb within 3–4 months to aggressive lymphomas [51].

Decorin is also involved in the regulation of angiogenesis [52,53] and blocks tumor cell-mediated angiogenesis by downregulating VEGFA production [54], as well as Met and downstream angiogenic networks [55]. Moreover, recombinant decorin proteoglycan or decorin protein core inhibits metastatic spreading of breast carcinoma xenografts [56,57]. Adenoviral-mediated decorin gene delivery and/or via systemic treatment retards the growth of various tumor xenografts including squamous, breast, and prostate carcinomas [32,42,56–62]. Low levels of decorin are present in invasive breast carcinomas [63] and this trait is associated with poor outcome in breast [64] and lung cancer patients [65]. Moreover, abnormal decorin expression has been detected in mammographic density [66], a major risk factor for breast cancer [67–69], and array data have demonstrated decorin upregulation during mammary gland involution, likely contributing to increased collagenization [70]. Thus, the expression and/or activity of decorin could affect breast cancer risk. Accordingly, any mechanism that would boost endogenous expression of decorin [71] or any therapeutic modality that could efficiently and specifically deliver decorin to carcinomas could represent a novel therapeutic choice against cancer [72,73].

Thus, we wished to deepen our molecular understanding of its potential role in modulating the tumor stroma by directly investigating, at high resolution, the gene expression signature of a triple negative breast carcinoma microenvironment. Therefore, for the first time, we were able to dissect the complex interrelationship present between the tumor and the stroma by utilizing a novel high-density microarray platform capable of simultaneously measuring expressed transcripts derived from both the mouse (i.e. the stroma) and the neoplasm (i.e. the human tumor cell line, MDA-MB-231) via interrogation of orthotopic tumor xenografts treated systemically with decorin.

In this study, we report the stromal gene expression signature obtained with systemic delivery of decorin protein core and

discover a total of 374 genes, which showed differential expression profiles. Further, and unexpectedly, we found by DAVID gene ontology analysis, a predominant inhibition of inflammatory and immune response genes with concurrent induction of various tumor suppressors and cellular adhesion molecules. Moreover, independent verification of the top 12 genes demonstrating  $>2$ -fold up or down regulatory changes identified *Mrgpra2*, *Siglech*, *Ing1* and *Il1b* to be potently suppressed concurrent with *Zc3hav1*, *Peg3*, and *Bmp2k* induction. These data posit for decorin protein core as a potent tumor repressor by attenuating inflammation and metastasis, which constitute several hallmarks of cancer.

## Results

### MDA-231(GFP+) Tumor Xenografts Respond to Systemic Delivery of Decorin

We performed experiments utilizing a very aggressive MDA-231(GFP+) triple-negative breast carcinoma cell line. We discovered that decorin evoked growth inhibition *in vitro*, enhanced apoptosis and blocked EGF- and FGF-mediated evasion from Matrigel (not shown), indicating that decorin exerts similar inhibitory activity on EGFR and Met dependent pathways as shown for other carcinoma cells [39,40,42,57]. Subsequently, we injected  $\sim$ 3 million MDA-231(GFP+) cells into the mammary fat pads of SCID mice (n=6 each), and when the tumor reached palpable size we treated them with daily i.p. injections of recombinant decorin protein core (10 mg/Kg). Purity of the preparation of decorin protein core was established by SDS polyacrylamide gel electrophoresis followed by staining with Colloidal Coomassie blue which can detect as little as 5 ng of protein. We did not find any co-purifying contaminants using this method (Figure S1). Therefore, based on this information, and since the largest amount of decorin protein core loaded was 5  $\mu$ g, our preparation of decorin protein core is  $>99\%$  pure. The results show that decorin protein core (henceforth designated decorin) was capable of retarding the growth of the breast carcinoma xenografts (Figure 1A–D), which was highly significant at day 23 (Figure 1B,  $P<0.001$ ). At the end of the experiments, the tumors were snap-frozen in liquid nitrogen and RNA was extracted for NimbleGen analysis.

### Analysis of Stromal (Mus Musculus) and Epithelial (Homo Sapiens) mRNA by the NimbleGen High-Density Mixed Expression Array Platform

To achieve a greater understanding of the governing interactions between the neoplastic cells and surrounding microenvironment we initially investigated the transcriptome of breast cancer stroma utilizing the orthotopic human mammary carcinoma xenografts described above. This approach is based on the utilization of a unique high-density microarray platform capable of differentiating and profiling transcripts from both human and mouse origin on the same array (NimbleGen 3 $\times$ 720 K). The mixed gene expression chip allows three arrays per slide with each array exhibiting 720,000 probes representative of transcripts originating from both human neoplastic cells and mouse stroma components. Appropriate sample labeling of the validated cDNA was followed by hybridization to the 3 $\times$ 720 K array followed by scanning using the Roche NimbleScan software, which normalizes the expression data using quantile normalization as determined by the Robust Multichip Average algorithm. Expression data were tested for significance using a mixed effects model ANOVA in R. Genes were sorted by  $P$ -value, and then by fold change. Genes with  $P<0.05$  were placed into upregulated and downregulated groups as illustrated with the resultant heat maps. We have

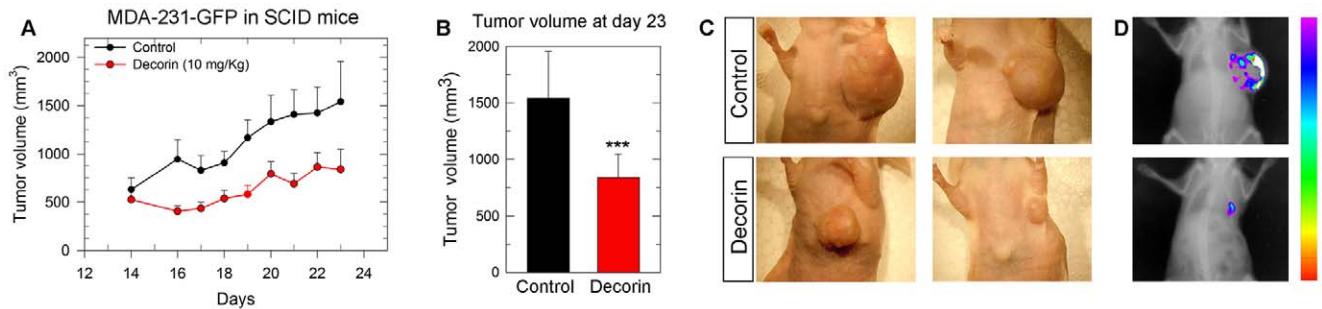


**Figure 1. Systemic delivery of decorin protein core inhibits the growth of orthotopic breast carcinoma xenografts.** **A:** Growth of MDA-231(GFP+) xenografts following daily i.p. injections of either PBS (black circle, control) or recombinant decorin protein core (red circle, 10 mg/kg). **B:** Tumor volumes at day 23, \*\*\* $P < 0.001$ . **C:** Representative macroscopic photographs of control and decorin-treated animals at day 23. **D:** Bioluminescence superimposed on x-ray analysis of a representative control and decorin treated animal at day 23. Images were captured with a Kodak In-Vivo Multispectral Imaging System FX. doi:10.1371/journal.pone.0045559.g001

deposited the results of the microarray data sets in the publically-available GEO System with accession number GSE37937. Global expression profiles comparing human breast carcinoma in decorin treated when compared to vehicle control showed that most of the genes in two independent experiments ( $n = 6$  each) showed close grouping with only minor changes (Figure 2A). Indeed, we found no significant ( $P < 0.05$ ) changes in any of the human-derived genes. In contrast, the number of genes derived from the tumor stroma of decorin-treated animals showed significant changes, with both upregulated and downregulated genes (Figure 2B). To further refine the search, we performed Principal Component Analysis and eliminated two outliers from each group. With this filtered set ( $n = 4$  each), we identified 374 differentially expressed genes with  $P < 0.05$ . Among all the genes, we selected the top 27 genes exhibiting greater than 2-fold down or upregulation and  $P < 0.01$ . Notably, these genes clustered very well (Figure 2C).

These findings show that systemic delivery of decorin in this triple-negative orthotopic breast carcinoma xenograft predominantly affects the global gene signature of the tumor microenvironment.

### Stromal Decorin Differentially Inhibits Expression of Immunomodulatory Genes and Concomitantly Induces Expression of Multiple Tumor Suppressor Genes

Gene ontology (GO) analysis was performed on the microarray data set comprising the 374 differentially expressed genes exhibiting  $P < 0.05$ . Utilization of the Database for Annotation, Visualization, and Integrated Discovery (DAVID v6.7) [74] allowed for a detailed ontology analysis based on the assigned cellular and molecular functions of the differentially regulated stromal genes in the presence of decorin. We thereby found the genes clustering into 5 discrete downregulated and 6 upregulated GO terms (Figure 3), associating with high significance values.

Remarkably, the leukocyte chemotactic and inflammatory genes represented the most significantly downregulated class ( $n = 63$ , enrichment score of 3.35,  $P = 0.0014$ ) among the differentially regulated stromal genes followed by contractile fiber genes and those responsible for orchestrating the general immune response (Figure 3). This representation of GO terms is appropriate and consistent as the most downregulated gene ( $-5.3$  folds), as determined by microarray analysis (cfr. Figure 2C), was immune response gene 1 (Irg1). Interestingly, full expression of Irg1 is dependent on estrogen signaling [75] and is a gene typically induced in macrophages by pro-inflammatory stimuli such as TLR agonists (lipopolysaccharide), IFN $\gamma$ , and TNF $\alpha$  [76,77]. It is

important to note that our MDA-231 orthotopic breast carcinoma models used for these studies are triple negative for ER $\alpha$ /PgR/HER2. Thus, these findings indicate an estrogen-independent mode of Irg1 downregulation via decorin. Importantly, and to the best of our knowledge, this gene has not previously been implicated in breast tissue and/or tumor progression and may serve as a novel component in tumorigenesis and detection.

Other suppressed immunomodulatory genes of interest included Siglech (Sialic acid binding Ig-like lectin;  $-2.3$  folds,  $P = 0.00844$ ), Lipg (IFN $\gamma$  inducible GTPase;  $-2.72$  folds,  $P = 0.0082$ ), and Il1b (Interleukin 1 $\beta$ ;  $-2.3$  fold,  $P = 0.0046$ ). Siglech is a member of the Ig gene superfamily, which binds avidly to sugars and is the mouse homologue of SIGLEC-15, the only known family member to maintain complete conservation throughout vertebrate evolution [78]. Lipg is a member of the small GTPase family of Golgi- and endoplasmic reticulum-associated subfamily activated primarily by TLR signaling and IFN $\gamma$  [79–81]. Finally, Il-1 $\beta$  is a primary mediator of innate and adaptive immune responses and has been firmly established as a regulator of cancer progression via control of proliferation and apoptotic processes [82].

Taken together, this signature of decorin-suppressed stromal genes indicates an immunosuppressive nature and constitutes a very poorly understood and under-investigated area of decorin bioactivity. However, recent publications are now positing a potent immunomodulatory role for decorin in various settings [83,84] and in tumorigenesis [85].

As for the stromal induced gene subsets, cell adhesion molecules commanded the majority as the most significantly enriched GO term ( $n = 282$ , enrichment score of 8.73,  $P = 0.00005$ ) followed by cytoskeletal components ( $n = 113$ , enrichment score of 2.78,  $P = 0.0032$ ), and cell cycle regulatory genes ( $n = 107$ , enrichment score of 1.88,  $P = 0.0036$ ) (Figure 3). The cellular and molecular functions these gene subsets represent are highly consistent for the ascribed properties of decorin functioning in a tumor repressive capacity as these classifications are associated with tumor suppressive activity.

The top stromal upregulated gene was a kinase induced by Bmp2, known as Bmp2 inducible kinase (Bmp2k). Bmp2k is a largely unknown and poorly investigated nuclear-localized serine/threonine kinase that represents another candidate gene not yet implicated in human breast cancer and might represent an important target for decorin bioactivity as well as a potentially novel biomarker for tumor progression.

Another decorin-induced stromal gene was cell adhesion molecule 1 (Cadm1,  $-2.7$  fold,  $P = 0.0011$ ), a transmembrane

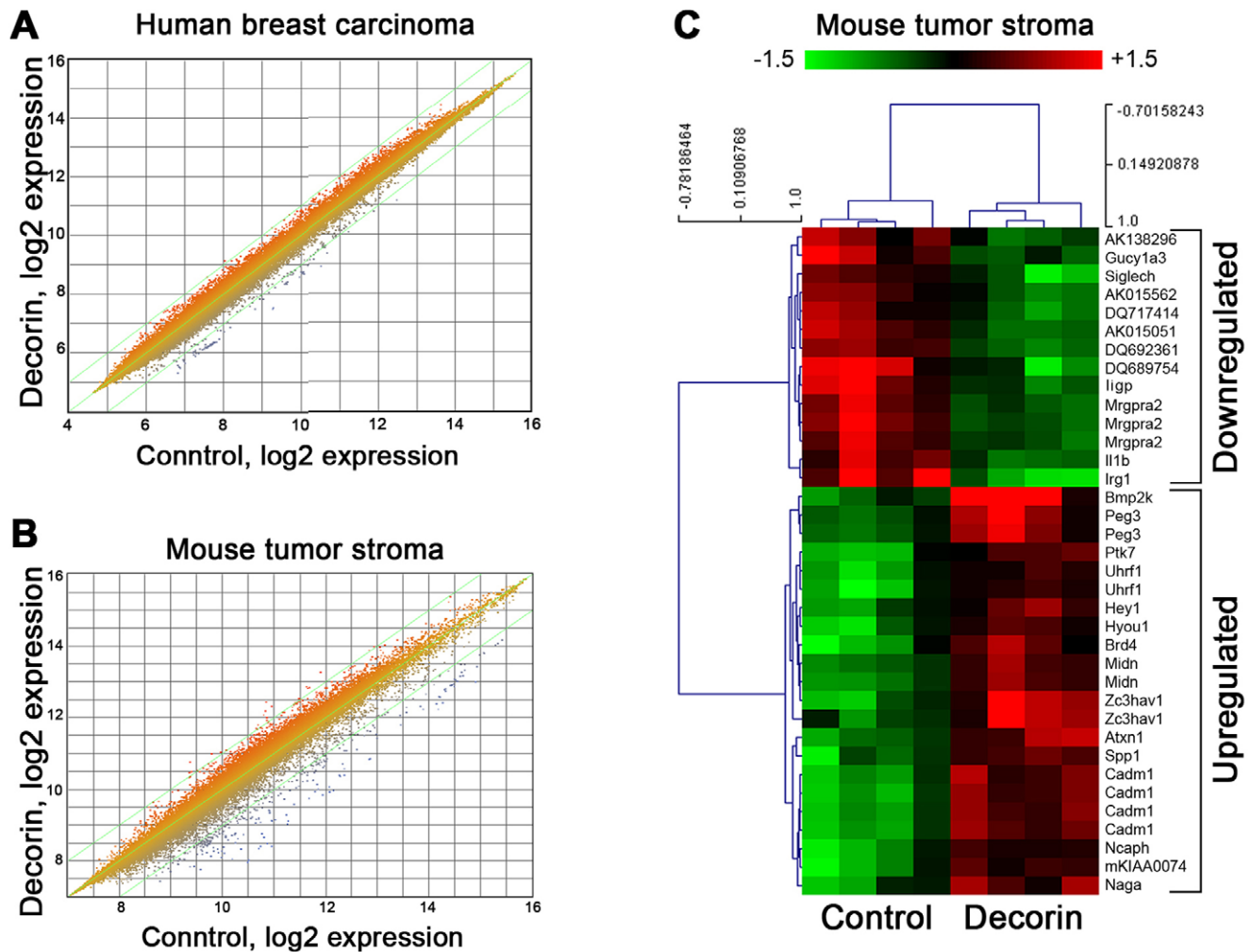


**Figure 2. Systemic delivery of decorin protein core alters the gene expression profile of the mammary tumor stroma xenografts.** **A,B:** Global expression profile comparing log<sub>2</sub> expression of vehicle control vs. decorin-treated tumor xenograft samples. Notice that the effects of decorin are more pronounced in the gene expression profile of the mouse-derived tumor stroma. **C:** Hierarchical clustering of the top 36 genes downregulated (n = 12) or upregulated (n = 15) in the mouse tumor stroma in control and decorin-treated mice. These 27 top genes were selected on the basis of two criteria: >2-fold change and  $P < 0.01$ . doi:10.1371/journal.pone.0045559.g002

glycoprotein containing Ig-like C2 modules in the ectodomain [86], also known as Tumor Suppressor in Lung Cancer (TSLC1). Expression of *Cadm1* is lost in various malignancies, including breast [87], due to promoter hypermethylation.

An additional decorin-induced target classified as a tumor suppressor gene within the stroma, was *Peg3* (paternally expressed gene 3, 2.49-folds,  $P = 0.0078$ ) and it encodes a zinc finger transcription factor (Cys<sub>2</sub>His<sub>2</sub> variety) of the Krüppel-type family. Similarly to *Cadm1*, this gene is also frequently silenced by promoter hypermethylation and/or loss of heterozygosity in several tumors including ovarian cancer [88] and gliomas [89].

The results derived from the DAVID gene ontology analysis provided a critical assignment of cellular and molecular function to our data subsets that are largely consistent with the top scoring genes as determined by the mixed microarray. These data suggest a novel role for decorin as a key immunosuppressive agent that is acting on the tumor stroma that may compromise the tumor-immune system interface, which is crucial for maintaining continued tumor progression. Simultaneously, decorin induces the expression of several tumor suppressor genes that, like several

of the downregulated targets, have never previously been linked to cancer progression.

#### Validation of Differentially-expressed Stromal Genes by Systemic Decorin Delivery

Independent verification of microarray datasets is absolutely critical for determining the validity and biological fitness of the presumed findings. Since the microarray platform was unique insofar as containing probes representing two different species and our data report the impact of decorin on stromal gene signatures (of *Mus musculus* origin) we therefore designed primers using the Universal Probe Library (Table S1) that are specific only for *M. musculus* transcripts, aimed at the top 6 up- and down-regulated (exhibiting  $P < 0.01$ ) stromal genes. Thereby, we have rigorously authenticated our primers in both *M. musculus* cDNA, harvested from NIH3T3 cells (positive control), and *Homo sapiens* cDNA as derived from HeLa cells (negative control for primer specificity). Our primers were capable of differentiating and recognizing only *M. musculus* mRNA species, in contrast to *H. sapiens* mRNA as validated by qPCR under identical thermal cycling conditions



Gene Ontology	Number of genes	Enrichment score	Mean $p$	Mean Benjamini (False Discovery Rate)
<b>Downregulated</b>				
Leukocyte chemotaxis & inflammation	63	3.35	0.0014686	0.053
Contractile fibers	32	2.8	0.0000472	0.00085
Immune response	11	1.83	0.000758	0.0271
Muscle contraction	7	2.64	0.00147	0.0533
Hormone regulation	3	1.57	0.00380	0.17
<b>Upregulated</b>				
Cell adhesion	282	8.73	0.00005312	0.00490
Cytoskeleton	113	2.78	0.003265	0.02145
Cell cycle regulation	107	1.88	0.00366055	0.1083
Lipid biosynthesis	51	2.35	0.00137911	0.08288
Phosphatases	28	1.66	0.0065	0.42
Vasculogenesis	20	1.95	0.0076	0.35

**Figure 3. DAVID gene ontology analysis.** Rigorous classification of the 374 differentially expressed genes within the tumor microenvironment of triple negative breast carcinoma xenografts following systemic treatment with decorin protein core for 23 days. Determinations for the down- and upregulated classes were selected on highly stringent criteria ( $P < 0.05$ ). Thus, all subsets above this value were analyzed by summing all genes within a specific gene ontology class followed by deriving the mean  $P$  and Benjamini values. doi:10.1371/journal.pone.0045559.g003

(Table 1). Further, eight of the twelve primer sets had no discernable amplification in *H. sapiens* when compared to *M. musculus* where a majority of the primer sets reported signal in the early to mid-range of thermal cycle 20. Thus, these data indicate high sensitivity with exquisite recognition and specificity for only *M. musculus* transcripts.

Utilizing mRNA extracted from the same tumor xenografts (systemic decorin treatment for 23 days at 10 mg/Kg) and that used for the microarray experiments, we performed qPCR as a

method to validate stromal gene expression for *Mrgpra2*, *Gucy1a3*, *Siglech*, *Ligp*, *Irg1*, and *Il1b* (downregulated genes) and for *Bmp2k*, *Cadm1*, *Hey1*, *Peg3*, *Brd4*, *Zc3hav1* (upregulated genes). We were able to recapitulate and confirm the gene expression signatures for four (~67%) of the downregulated genes (*Mrgpra2*, *Siglech*, *Irg1*, and *Il1b*;  $P < 0.001$ ) and for three (50%) of the upregulated genes (*Zc3hav1*, *Peg3*, and *Bmp2k*;  $P < 0.001$ ) (Figure 4). The remaining genes (*Cadm1*, *Hey1*, *Brd4*, *Gucy1a3*, and *Ligp*) could not be faithfully reproduced due primarily to unfavorably high thermal cycle value

**Table 1.** Demonstration that qPCR verification primers exhibit exquisite specificity for NIH3T3 (mouse embryonic fibroblasts) cDNA when directly compared to HeLa (human squamous cell carcinoma) cDNA.

Official Gene Symbol	HeLa cDNA Average Ct ( $\pm$ S.D.)	NIH3T3 cDNA Average Ct ( $\pm$ S.D.)	Average $\Delta$ Ct (HeLa - NIH3T3 Ct)
Bmp2k	32.92 ( $\pm$ 0.18)	26.03 ( $\pm$ 0.16)	6.89
Mrgpra2	36.57 ( $\pm$ 0.36)	28.28 ( $\pm$ 0.38)	8.29
Cadm1	Not Detected	37.40 ( $\pm$ 0.16)	N/A
Hey1	Not Detected	31.52 ( $\pm$ 0.49)	N/A
Gucy1a3	35.88 ( $\pm$ 0.70)	28.33 ( $\pm$ 0.27)	7.55
Peg3	Not Detected	25.41 ( $\pm$ 0.17)	N/A
Brd4	37.25 ( $\pm$ 0.33)	22.58 ( $\pm$ 0.02)	14.67
Zc3hav1	Not Detected	25.36 ( $\pm$ 0.20)	N/A
Siglech	Not Detected	29.67 ( $\pm$ 0.12)	N/A
Ligp	Not Detected	33.17 ( $\pm$ 0.14)	N/A
Irg1	Not Detected	34.83 ( $\pm$ 4.26)	N/A
Il1b	Not Detected	26.49 ( $\pm$ 1.00)	N/A

Average Ct ( $\pm$  S.D.) values were obtained via qPCR for each gene primer set listed above when exposed to either NIH3T3 or HeLa template cDNA following standard 40 cycle SYBR Green evaluation as performed on the Roche 480 LightCycler II platform in either quadruplicate (HeLa) or triplicate (NIH3T3). HeLa Ct values scored as "Not Detected" refers to either all four replicates failing to register a detectable amplicon threshold or reflects that only one replicate achieved threshold detection, which most likely reflects stochastic amplicon formation at higher Ct values ( $> 35$ ); further, values that surpassed a Ct of 35 were considered as "Not Detected".

doi:10.1371/journal.pone.0045559.t001

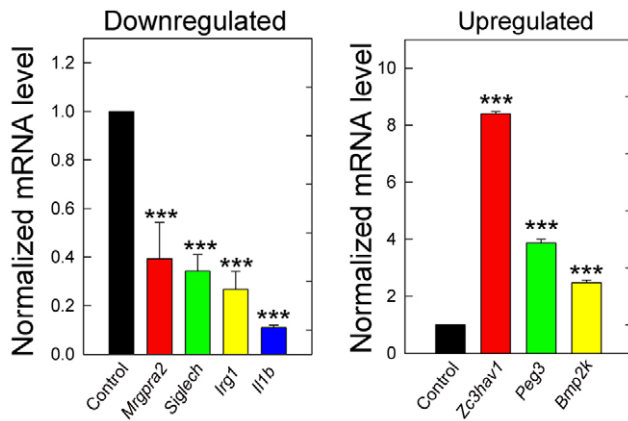


**Figure 4. Independent qPCR verification of NimbleGen targets in orthotopic MDA-231 tumor xenografts following systemic delivery of human recombinant decorin protein core.** Of the 36 top scoring candidates, we selected the top six-upregulated and downregulated targets and verified the corresponding expression patterns independently via real time quantitative PCR (qPCR) analysis on the same MDA-231 tumor xenograft total RNA utilized for the NimbleGen Mixed expression array. Since these 12 candidate genes represent differential stromal (mouse) gene expression signatures, we ensured our primers exhibit extreme stringency and specificity for only *Mus musculus* transcripts (*cf.* Table 1). Therefore, we were able to demonstrate reproducibility and verification for seven of the twelve candidate genes, representing four downregulated (*Mrgpra2*, *Siglech*, *Irg1*, *Il1b*) and three upregulated (*Zc3hav1*, *Peg3*, *Bmp2k*) transcripts in our MDA-231 xenograft mouse model. Data are representative of three independent samples for each sample cohort in quadruplicate replicates, analyzed with the  $\Delta\Delta C_t$  method (please see Materials and Methods for a more detailed explanation), and reported as the average fold change  $\pm$  SEM ( $***P<0.001$ ). doi:10.1371/journal.pone.0045559.g004

or lack of amplification and detection under the cycling conditions employed, suggesting low transcript number.

These data suggest a modulation of immunological genes, consistent with the aforementioned DAVID gene ontology analysis. Importantly, we demonstrate a reproducible induction of a presumed tumor suppressor gene (*Peg3*) within the stromal compartment as well as implicating a novel role for *Bmp2k* in breast cancer samples.

#### Co-Cultures Mimic Decorin Regulated Stromal Genes In Vitro

We hypothesized that establishment of a co-culture approach could reconstitute in part the decorin-evoked *in vivo* stromal gene expression signatures obtained from the tumor xenografts in an *in vitro* setting. Thus, we utilized primary cell isolates of mouse mammary fibroblasts of the same genetic background (C57BL/6J) as the host for the tumor xenografts and added human mammary carcinoma MDA-231 cells to this feeder layer of primary mammary fibroblasts. Once attached, co-cultures were serum starved for 24 hours followed by chronic treatment with decorin (100 nM) for 3 days whereupon RNA was harvested and prepared as a mixed cDNA population. We focused on the expression pattern of the seven previously verified genes as reported above. Analysis of these stromal genes in context of the co-culture via qPCR revealed a recapitulation of the expression patterns of *Peg3*, *Bmp2k*, and *Zc3hav1* (Figure 5;  $P<0.001$ ), the same stromal genes verified as induced by decorin within the tumor xenografts. However, the extents of induction among these genes were not as dramatic as shown for the verification *in vivo* (*cf.* Figure 4). This

#### Co-Culture Expression Verification

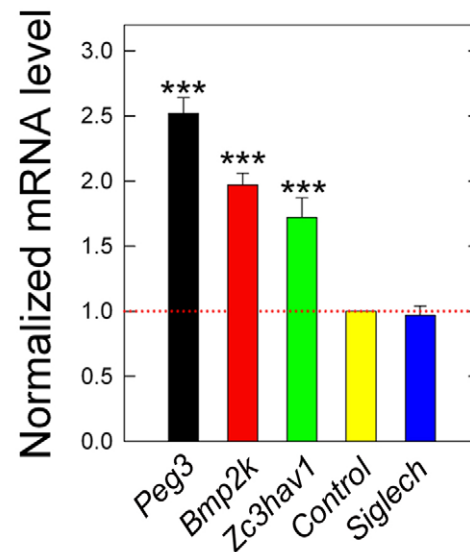


**Figure 5. Co-Culture Gene Expression Analysis of NimbleGen Targets.** Co-culture conditions were established by utilizing and plating primary mouse mammary fibroblasts followed, once at sub-confluency, by the addition of  $\sim 10^5$  MDA-231 cells. Co-cultures were then serum starved for a 24 h period prior to exposure of 100 nM decorin protein core for a total 3–4 days under serum free conditions. Gene expression analysis was carried out via qPCR by employing the same *Mus musculus* specific primers as in the preceding section for seven of the target genes, as were reproduced in Figure 4. Recapitulation of the *in vivo* gene signature involved reproducible patterns for four of the genes (*Peg3*, *Bmp2k*, and *Zc3hav1*). Data are representative of two independent trials performed in quadruplicate replicates and analyzed with the  $\Delta\Delta C_t$  method (Please refer to Materials and Methods) and reported as the average  $\pm$  SEM ( $***P<0.001$ ). doi:10.1371/journal.pone.0045559.g005

reflects several possibilities such as the length of decorin treatment, differences in nutrient obtainment via the blood vessels and/or the lack of additional stromal cells (endothelial cells and inflammatory cells), which might synergize and ultimately prove necessary for more robust decorin-mediated induction.

It is of note to mention that expression patterns of the immunomodulatory genes could not be reconstituted since our cultures lacked immune system components and/or fibroblasts that do not normally express these genes. Finally, and although *Siglech* was highly detectable within our co-culture system, we found no significant change of its expression (Figure 5;  $P>0.05$ ).

Collectively, these findings indicate that decorin is capable of targeting the tumor stroma in addition to the well-established anti-oncogenic activity targeting the carcinoma cells.

#### Decorin Induces *Peg3*, *Bmp2k* and *Zc3hav1* in a Co-culture and Tumor Xenografts

Following extensive qPCR analyses, we next sought to determine the levels of *Peg3* and *Bmp2k* in a co-culture of mouse mammary fibroblasts and MDA-231 that were exposed to either vehicle (control) or decorin (200 nM) for up to 3 days. We found a marked increase of both *Peg3* and *Bmp2k* expression in treated cells compared to controls as detected by immunoblot (Figure 6). To further strengthen the *in vivo* relevance of our data, we determined the expression of *Peg3* and *Bmp2k* in the same

orthotopic mammary tumor xenografts as used above. Systemic treatment with decorin resulted in an induction of Peg3 (Figure 7A) as well as Bmp2k (Figure 7B) and Zc3hav1 (Figure S2) within the tumor stroma as visualized via immunofluorescence and quantified using three-dimensional surface plots of the fluorescent signal. Thus, these *in vivo* data provides further proof that decorin significantly affects the tumor microenvironment via induction of Peg3, Bmp2k and Zc3hav1 at the protein and transcriptional levels as suggested by the mixed microarray data.

### Invasive Ductal Breast Carcinoma Microarray Datasets Show a Clear Reduction in PEG3

Next, we analyzed *PEG3* expression in different publically available breast cancer microarray datasets using the ONCOMINE database and gene microarray data analysis tool [90]. This database was specified to query individual published microarray analyses as well as to produce a summary statistic across each distinctive gene expression study for *PEG3* mRNA levels detected in various ductal breast carcinoma samples. Two independent studies [91,92] demonstrated a statistically significant decrease (Figure 8) of *PEG3* mRNA expression when compared to normal, non-neoplastic controls. Precisely, the dataset by Karnoub *et al.* reported a 3.1-fold decrease ( $P=3.6\times 10^{-6}$ ) of *PEG3* mRNA within invasive ductal breast carcinoma (Figure 8, left panel) which is consistent with a study by Richardson *et al.*, where a 5.6-fold reduction ( $P=1.86\times 10^{-6}$ ) of *PEG3* expression was found in ductal breast carcinoma (Figure 8, right panel). No data were available in the ONCOMINE for either *BMP2K* or *ZC3HAV1* related to breast cancer.

These data provide further *in vivo* validation concerning the clinical relevance and potentially critical role of PEG3, functioning as a tumor suppressor, in the progression of aggressive ductal breast carcinomas. Moreover, these studies provide strong rationale for the novel induction of PEG3 within this malignancy by decorin as a possible mechanism of inhibiting tumorigenesis.

### Discussion

A current prevailing view is that tumor-associated stroma is activated by cancer cells to foster tumor growth by secreting

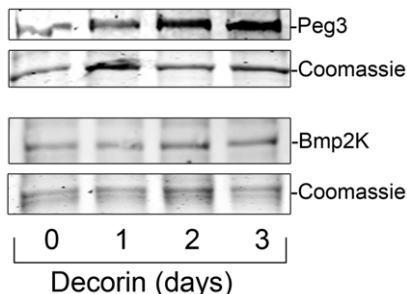


**Figure 6. Peg3 and Bmp2 expression is induced by decorin protein core in co-cultures of MDA-231 cells and mouse mammary fibroblasts.** Representative immunoblots of MDA-231 cells and mouse mammary fibroblasts in co-culture exposed to 200 nM decorin as indicated. Cell lysates were separated via SDS-PAGE and immunoblotted using an anti-Peg3 or Bmp2k primary antibodies. The bottom panels represent Coomassie Blue staining of the lower portion of the gel. The blots are representative of three independent experiments. Proteins were visualized with IR-Dye-labeled secondary antibodies and quantified using Odyssey Infrared Imaging system (LICOR).

doi:10.1371/journal.pone.0045559.g006

growth factors, enhancing angiogenesis, and facilitating cell migration, ultimately culminating in metastasis to remote organ sites [93–97]. Thus, genes mediating tumor-stroma interactions could provide novel targets for diagnostic development and therapeutic intervention [98]. Exploratory genome-wide analysis of the tumor microenvironment in breast cancer has been limited to date. Using serial analysis of gene expression coupled with antibody-based *ex vivo* tissue fractionation, Polyak and co-workers identified 417 cell-type-specific genes among the most prominent cell types in breast cancer [97]. They demonstrated gene expression alterations in all cell types within the tumor microenvironment accompanying progression from normal breast tissue to ductal carcinoma *in situ* (DCIS) to invasive ductal carcinoma (IDC), providing evidence that these cell types all participate in tumorigenesis. Park and colleagues more recently obtained gene expression profiles of both epithelial and stromal compartments from the same tumor biopsy using laser capture microdissection (LCM) and described a stromal gene expression profile capable of predicting clinical outcome [99]. Further, using LCM, Sgroi and colleagues discovered that most of the gene expression changes take place prior to local invasion and, surprisingly, no major changes in gene expression accompanying the *in situ*-to-invasive growth transition [100].

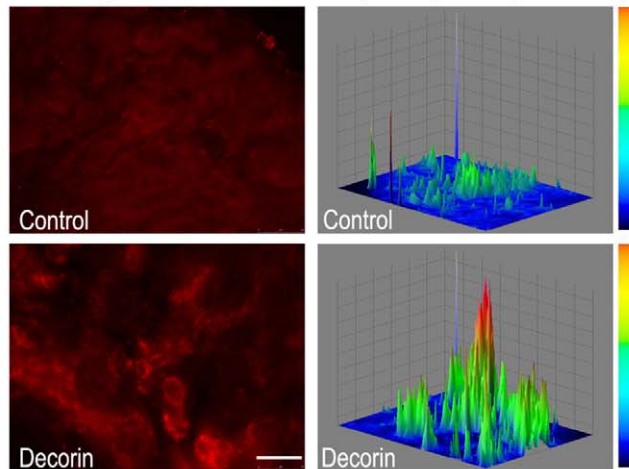
Similarly, analysis of the tumor microenvironment by the same authors revealed, in analogy to the epithelium, that the tumor stroma undergoes extensive gene expression alterations even at the pre-invasive stage of DCIS, supporting the view that paracrine mechanisms play an important role [101]. The observed gene expression changes in the stroma associated with DCIS and IDC suggests coevolution of the tumor stroma with the tumor epithelium prior to tumor invasion.

The anti-tumorigenic properties of decorin have been presented as a stromally derived tumor repressor that functions by directly binding to receptor tyrosine kinases situated on the tumor cell membrane [73]. Recently it has been shown that this mechanism allows decorin to target potent oncoproteins such as  $\beta$ -catenin and Myc for degradation while presumably rendering large genetic networks that would otherwise favor continued tumorigenic growth, vulnerable to changes in gene expression signatures that would foster a less malignant state [49]. Analogously, and since decorin is a putative matrix constituent and functions as a soluble paracrine factor on the tumor proper, we sought to identify gene network changes within the broader context of the tumor microenvironment, as this compartment co-evolves with the tumor, following systemic decorin treatment on triple-negative orthotopic breast carcinoma xenograft to gain a better understanding of the molecular interplay evoked by decorin.

We found that soluble decorin protein core, acting in a paracrine capacity, is capable of substantially altering the stromal gene signature as evidenced by the differential modulation of 374 stromal genes. Gene ontology analysis revealed unexpected enrichments for suppressed genes constituting immune responses while concomitantly inducing cell adhesion and tumor suppressor genes.

Subsequently, the array yielded reproducible signatures for *Mrgpra2*, *Siglech*, *Irg1*, and *Il1b* (downregulated subset) and *Peg3*, *Bmp2k*, and *Zc3hav1* (induced subset). Establishment of co-cultures (primary mouse mammary fibroblasts and MDA-231 cells) allowed recapitulation of the mRNA expression pattern of the upregulated genes only; our co-culture models lacked immune-competent cells, thus the downregulated subset was not detected. Seemingly, our data presented above seem to contradict a recently published article indicating that decorin advocates for a more pro-inflammatory tumor microenvironment [85]. Only intact decorin

**A Peg3 levels in MDA-231 (GFP+) xenografts**



**B Bmp2k levels in MDA-231 (GFP+) xenografts**

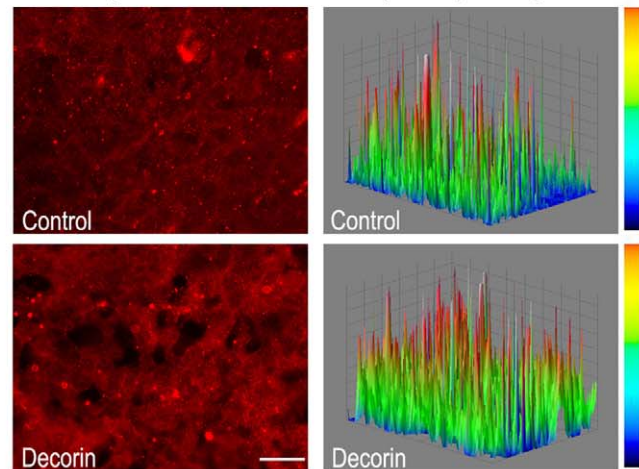


**Figure 7. Systemic administration of decorin protein core induces Peg3 and Bmp2k levels in MDA-231(GFP+) xenografts. A–B:** Immunofluorescence images of control and decorin-treated MDA-231(GFP+) tumor xenografts, reacted with anti-Peg3 (A) or anti-Bmp2k (B) antibodies. Mice bearing MDA-231(GFP+) tumor xenografts were treated with intraperitoneal injection of decorin protein core (10 mg/kg) every other day for 23 days. All the micrographs were taken using the same exposure and gain. Three-dimensional surface plots, on the right of each panel, were generated utilizing ImageJ software and represent Peg3 and Bmp2k expression which directly corresponds to the signal intensity obtained by the immunofluorescence. The scale bars for signal intensity are included on the right of each surface plot. Bar = 20 μm.  
doi:10.1371/journal.pone.0045559.g007

proteoglycan, not the protein core, is able to trigger the release of TNFα or IL-12p70 from macrophages [85]. The binding of decorin protein core to TLR2/4 is not sufficient to evoke downstream signaling events, which is in contrast to decorin proteoglycan. Therefore, since our present study utilized decorin protein core, the results obtained are compatible and do not contradict. Importantly, the mRNA data for *Peg3*, *Bmp2k*, and *ζc3hav1* were independently corroborated via immunofluorescence and immunoblotting in not only tumor xenografts but also in co-culture conditions, respectively, and revealed, for the first time, a novel role for *Peg3*, *Bmp2k*, and *ζc3hav1* in breast cancer progression.

*Peg3* represents a unique and distinctive class among the repertoire of inherited genes by virtue of its genomically imprinted status, where in this case, the paternal allele is exclusively responsible for expressing a molecule which harbors 12 Krüppel-type zinc finger domains with two proline-rich periodic repeat domains, and is frequently rendered inactive in several malignancies [88,89]. Consistent with a potential role as a tumor suppressor and in line with recent publications from our lab, it has been experimentally shown [102] that the N-terminal SCAN domain of *Peg3* mediated direct binding to β-catenin and promotes 26S proteasomal degradation that is, surprisingly, independent of GSK3β. These studies phenocopy the pathway utilized by decorin

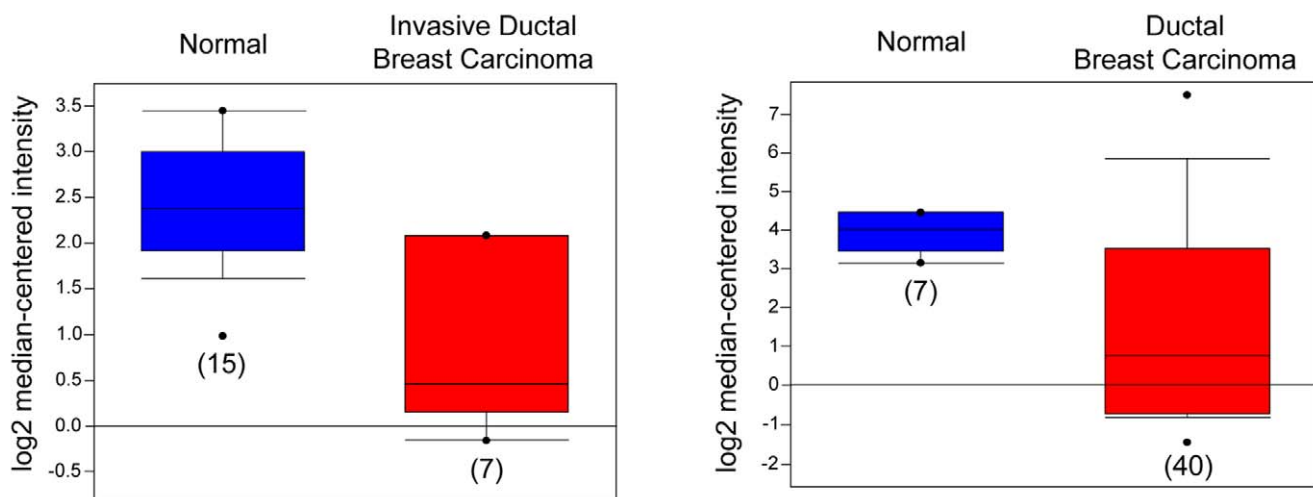


**Figure 8. Expression array analysis of several ductal breast carcinoma microarray datasets.** Statistical significance is reported as a summary statistic calculated utilizing the ONCOMINE gene expression tool [90]. As shown in the report by Karnoub *et al.* [91] (left panel) there was a 3.1-fold reduction of PEG3 mRNA within invasive ductal breast carcinoma ( $P = 3.64 \times 10^{-6}$ ). Additionally, in the study by Richardson *et al.* [92] (right panel), PEG3 levels were found to be decreased by 5.6-fold in ductal breast carcinoma samples ( $P = 1.86 \times 10^{-6}$ ).  
doi:10.1371/journal.pone.0045559.g008



for the non-canonical, GSK3 $\beta$ -independent antagonism and cessation of  $\beta$ -catenin signaling [40] and could provide a vital link between attenuation of RTK signaling and non-canonical  $\beta$ -catenin antagonism. Additionally, Peg3 has been shown to interact with and modulate the Bax/p53 axis, in concert with the TNF $\alpha$  and Wnt-related pathways as a mechanism to promote apoptosis [103].

Our second candidate gene is Bmp2k, a poorly understood serine/threonine kinase that plays a role in skeletal development where activation of Bmp2k is able to attenuate osteocalcin expression concomitant with reduced osteoblast differentiation [104]. Intriguingly, Bmp2k has a glutamine-rich region that shares homology to the trans-activation domain common to many transcription factors [104]. FoxC1, a transcription factor belonging to the forkhead superfamily, is subsequently able to induce the expression of Bmp2k [105]. In a separate pathological setting, a *BMP2K* variant, was reported to be strongly correlated with the development of high myopia [106].

Lastly, we were able to confirm induction of Zc3hav1 (also known as ZAP for zinc-finger antiviral protein), a gene hypothesized to encode CCCH-type zinc finger that is largely thought to prevent viral infection by retroviruses [107], particularly that triggered by HIV-1 [108]. This has novel implications on the postulated effector functions of Zc3hav1, in response to decorin, as it comprises a link to modulate innate cellular defenses against viral infections, and/or a mechanism to regulate endogenous RNA signaling within the tumor microenvironment.

Moreover, the data obtained from our co-culture suggests a potent modulatory effect on cancer-associated fibroblasts that will have a broad impact on tumor progression. Therefore, the changes in differential expression, as reported above, reflect gene signatures operative within the tumor microenvironment and thus makes assessing whether or not these changes are the result of direct effects on the tumor proper difficult. Thus, excluding the possibility of decorin protein core signaling via the fibroblast  $\alpha$ 2 $\beta$ 1 integrin receptor, it is plausible that decorin is targeting the tumor cells directly by suppressing EGFR and Met signaling (or is integrated over several receptors), and thereby functions as a paracrine agent to elicit changes within the surrounding tumor stroma. However, this model cannot exclude decorin binding directly to receptor tyrosine kinases within the stroma (such as receptors present on endothelial cells). Importantly, we have reported that decorin severely inhibits Myc function through targeted proteasomal degradation [40] which, in turn, could have stern consequences for the tumor stroma as a favorably pro-tumorigenic environment as Myc is required for the expression of stromal genes [109]. As an alternative possibility, it would be possible through the established role of decorin in sequestering and thus indirectly inhibiting the activity of TGF $\beta$ , to elicit the immunomodulatory changes in this manner [110].

In conclusion, validation of the mixed microarray data as it pertains to stromal gene changes via several experimental methodologies performed *in vitro* and *in vivo* revealed and confirmed a novel involvement for Peg3, Bmp2k, and Zc3hav1, for the first time, in breast carcinomas where, future studies may reveal direct functions related to modulating the surrounding tumor environment as dictated by decorin. These findings provide a new paradigm for decorin protein core in controlling the tumor microenvironment as a fundamental biological mechanism with great implications for curbing tumorigenic growth by the induction of novel tumor suppressor genes within the stroma and for the discovery of novel gene signatures that could eventually help clinical assessment and prognosis.

## Materials and Methods

### Ethics Statement

All animal studies were approved by the Institutional Review Board of Thomas Jefferson University. At the end of each experiment, mice were anesthetized with isoflurane and euthanized with CO<sub>2</sub> in accordance with institutional guidelines. (Approved Protocol # 196 G).

### Cells and Materials

MDA-MB-231 triple-negative breast carcinoma cells were obtained from American Type Culture Collection (Manassas, VA). MDA-231(GFP+) were previously described [111]. Cells were maintained in Dulbecco's modified Eagle's medium supplemented with 10% fetal bovine serum (FBS) (SAFC Biosciences, Lenexa, KS) as well as with 100  $\mu$ g/ml of penicillin/streptomycin (MediaTech, Manassas, VA). Primary antibody against Peg3 (ab99252) was from Abcam Inc. (Cambridge, MA); anti-Bmp2k polyclonal antibody (PA5-11724) was from Thermo Scientific (Rockford, IL); anti-Zc3hav1 polyclonal antibody was from Abgent (San Diego, CA).

### Purification of Decorin Protein Core

Decorin protein core was purified as described elsewhere [56]. Briefly, recombinant human decorin was expressed in 293-EBNA cells as a fusion protein to poly-His<sub>6</sub> within a Celligen Plus bioreactor [17]. The 293-EBNA cells were subsequently serum starved for several days in order to maximize the output of decorin in the media prior to purification. Under these conditions, the 293-EBNA cells will produce both the glycanated and unglycanated form of the recombinant decorin protein. Exploiting this method, it was possible to purify both the proteoglycan and protein core on an Ni-NTA chelating column followed by elution in increasing concentrations of imidazole (0 to 250 mM) in 20 mM Tris-HCl, 500 mM NaCl, 0.2% CHAPS, pH 8.0. Finally, the proteoglycan and core protein were separated via anion-exchange chromatography performed on Q-Sepharose and the expected doublet of decorin protein core was seen migrating with a molecular mass of  $\sim$ 50 kDa [112]. Additional evidence concerning the purity of the decorin protein core preparation used was provided via an SDS-PAGE gel to analyze increasing amounts (0.5, 1, 2, and 5  $\mu$ g) of decorin protein core in parallel with increasing amounts of bovine serum albumin (BSA) (2 and 5  $\mu$ g). This was followed by staining the resultant gel with colloidal Coomassie blue (EZBlue<sup>TM</sup> Gel Staining Reagent, Sigma-Aldrich), which has a detection threshold of as little as 5 ng of total protein.

### Generation of Tumor Xenografts

All the animal studies performed were approved by the Institutional Review Board of Thomas Jefferson University. Twelve severe-combined immunodeficient (SCID) hairless female mice (Charles River Lab., Malvern, PA) were injected with  $2 \times 10^6$  MDA-231(GFP+) cells into the upper left mammary fat pad. Two weeks later, once tumors were established, mice were randomized into two groups. Half the mice received a daily intraperitoneal injection of recombinant protein core (10 mg/Kg). The controls received 100  $\mu$ l of PBS. Three independent experiments were performed. Tumor growth was measured every day with a micro-caliper according to the following formula:  $V = a(b^2/2)$ , where  $a$  and  $b$  represent the larger and smaller diameters of the tumor, respectively. At the end of the experiment (day 23) mice were taken to the Small Animal Imaging Facility of Thomas Jefferson University and *in vivo* expression of GFP within the xenografts was analyzed with a Kodak In-Vivo Multispectral Imaging System FX.

Soon after all animals were sacrificed and all major organs were dissected and fixed in formalin, whereas tumors were cut in half and one half was snap-frozen in liquid nitrogen subsequent to RNA extraction whereas the other half was embedded in OCT compound (x) and frozen at  $-20^{\circ}\text{C}$ . 10  $\mu\text{m}$  thick cryostat sections were cut from the blocks and mount on superfrost slides which were then subjected to immunofluorescence staining.

### Immunofluorescence Staining of Tumor Sections

Immunofluorescence studies were performed as described before [40,113,114]. Frozen tissue sections of xenografts were fixed in ice cold acetone for 10 minutes. After blocking with 1% BSA,  $1\times$  PBS, sections were incubated with primary antibody against Peg3, Bmp2k or Zc3hav1 for 1 hour at room temperature. Sections were then probed with goat anti-rabbit IgG Alexa Fluor<sup>®</sup> 594 (Invitrogen). Washed sections were mounted with Prolong Gold (Invitrogen) and visualized using a Leica DM5500B microscope with Advanced Fluorescence 1.8 software (Leica Microsystems, Inc.). All the images were analyzed with Adobe Photoshop CS3 (Adobe Systems, San Jose, CA). Three-dimensional surface plots were generated utilizing ImageJ software.

### Isolation of Mouse Mammary Fibroblasts and Co-culture Experiments

Female wild type C57BL/6J mice were used to isolate primary mammary fibroblasts. Briefly, the fourth and fifth mammary glands were removed aseptically and minced with surgical blades. All the fragments were collected and diluted in 10 ml of digestion media (DMEM, 2 mg/ml collagenase type I, 50  $\mu\text{g}/\text{ml}$  gentamicin) and incubated in a shaker (2 hours at  $37^{\circ}\text{C}$ ) with gentle shaking. The solution was then centrifuged 10 minutes at 1000 rpm in order to eliminate floating fat cells. The obtained pellet was washed twice in 10 ml growth media (DMEM, 10% fetal bovine serum, pen/strep) containing fungizone. The cell pellet was then disaggregated by gently pipetting up and down with a 1 ml pipette tip. The cell resuspension was plated in 6-cm<sup>2</sup> dishes coated with gelatin and cultured in growth media containing fungizone. After a week, the fibroblast culture was switched to growth media and passaged accordingly.

For co-culture experiments, sub-confluent primary cultures of mouse mammary fibroblasts were seeded with  $1.0\text{--}1.5\times 10^5$  MDA-231 mammary carcinoma cells. The co-cultures were allowed to incubate for several hours for engagement of the fibroblast feeder layer. Co-cultures were then serum starved overnight whereupon chronic decorin treatment (100 nM decorin protein core) began for a total of three days. Arrival of the end-point resulted in lysing of the co-cultures in either a sufficient volume of RIPA buffer for immunoblot analyses or TRIzol (Invitrogen) to isolate total RNA and subsequent cDNA synthesis for gene expression analysis.

### Real-Time Gene Expression Verification and Analysis

Independent authentication of gene expression analysis was carried out by quantitative real-time polymerase chain reaction (qPCR) to confirm gene changes. Briefly, for *in vivo* samples, MDA-231 tumor xenografts tissue samples treated systemically with decorin protein core (10 mg/kg) for 23 days were snap-frozen with liquid nitrogen and homogenized with a mortar and pestle prior to solubilization in 2 ml of TRIzol (Invitrogen, Grand Island, NY), or alternatively, at the end point of the co-cultures (following three days of chronic 100 nM decorin protein core exposure), 6-cm<sup>2</sup> dishes were lysed in 2 ml of TRIzol. Subsequently, isolated total RNA (1  $\mu\text{g}$ ) was annealed with oligo(dT) primers, and cDNA was

synthesized utilizing the SuperScript Reverse Transcriptase II (Invitrogen) according to the manufacturer's instructions. Gene-specific primer sets for *Mus musculus* mRNA (refer to Table S1 and Table 1) were rigorously designed and verified prior to use in qPCR. Target genes and the endogenous housekeeping gene, *Actb*, amplicons were amplified in independent reactions using Brilliant SYBR Green Master Mix II (Agilent Technologies, Cedar Creek, TX). All samples were run in triplicate with quadruplicate plate replicates on the Roche LightCycler 480-II Real Time PCR platform (Roche, Madison, Wisconsin) and the cycle number (Ct) was obtained for each independent amplicon reaction followed fold change determination via the Comparative Ct method for gene expression data analysis. Delta Ct ( $\Delta\text{Ct}$ ) values are representative of normalized gene expression levels with respect to *Actb*. The delta delta Ct ( $\Delta\Delta\text{Ct}$ ) values represent experimental cDNA (samples treated with decorin protein core) minus the corresponding  $\Delta\text{Ct}$  of the calibrator sample (control samples). Finally, the reported fold change represents an average of the fold changes as calculated using the double  $\Delta\text{Ct}$  method ( $2^{-\Delta\Delta\text{Ct}}$ ).

### Supporting Information

**Figure S1 SDS-PAGE gel demonstrating the purity of the decorin protein core preparation.** SDS-PAGE gel representing increasing amounts (0.5, 1, 2, and 5  $\mu\text{g}$ ) of decorin protein core run in parallel with increasing amounts of BSA (2 and 5  $\mu\text{g}$ ), as indicated. The gel was subsequently stained with colloidal Coomassie blue for highly sensitive detection (as low as 5 ng) of any co-purifying bands in the decorin protein core preparation used. The left lane indicates the migration of the molecular mass (kDa) of standard proteins.

(TIF)

**Figure S2 Systemic administration of decorin protein core induces Zc3hav1 levels in MDA-231(GFP+) xenografts. A–B:** Immunofluorescence images of control and decorin-treated MDA-231(GFP+) tumor xenografts, reacted with an anti-Zc3hav1 antibody. Mice bearing MDA-231(GFP+) tumor xenografts were treated with intraperitoneal injection of human recombinant decorin core protein (10 mg/kg) every other day for 23 days. All the micrographs were taken using the same exposure and gain. Three-dimensional surface plots, on the right of each panel, were generated utilizing ImageJ software and represent Zc3hav1 expression which directly corresponds to the signal intensity obtained by the immunofluorescence. The scale bars for signal intensity are included on the right of each surface plot. Bar = 20  $\mu\text{m}$ .

(TIF)

**Table S1 Primer pairs specific for the exclusive detection of *Mus Musculus* genes with accompanying gene symbol and NCBI accession number.**

(DOCX)

### Acknowledgments

We thank Hannah Painter for help during the initial stages of this work.

### Author Contributions

Conceived and designed the experiments: RVI SB TN. Performed the experiments: SB TN. Analyzed the data: RVI SB TN GP RV BE LS Z-XW. Contributed reagents/materials/analysis tools: RTO LAI SCP Z-XW. Wrote the paper: RVI SB TN.

## References

- Theocharis AD, Tzanakakis G, Karamanos NK (2010) Proteoglycans in health and disease: Novel proteoglycan roles in malignancy and their pharmacological targeting. *FEBS J* 277: 3904–3923.
- Edwards IJ (2012) Proteoglycans in prostate cancer. *Nat Rev Urology* 9: 196–206.
- Danielson KG, Fazzio A, Cohen I, Cannizzaro LA, Eichstetter I, et al. (1993) The human decorin gene: intron-exon organization, discovery of two alternatively spliced exons in the 5' untranslated region, and mapping of the gene to chromosome 12q23. *Genomics* 15: 146–160.
- Santra M, Danielson KG, Iozzo RV (1994) Structural and functional characterization of the human decorin gene promoter. A homopurine-homopyrimidine S1 nuclease-sensitive region is involved in transcriptional control. *J Biol Chem* 269: 579–587.
- Mauviel A, Korang K, Santra M, Tewari D, Uitto J, et al. (1996) Identification of a bimodal regulatory element encompassing a canonical AP-1 binding site in the proximal promoter region of the human decorin gene. *J Biol Chem* 271: 24824–24829.
- Adany R, Iozzo RV (1990) Altered methylation of versican proteoglycan gene in human colon carcinoma. *Biochem Biophys Res Commun* 171: 1402–1413.
- Adany R, Iozzo RV (1991) Hypomethylation of the decorin proteoglycan gene in human colon cancer. *Biochem J* 276: 301–306.
- Coppock DL, Kopman C, Scandalis S, Gilleran S (1993) Preferential gene expression in quiescent human lung fibroblasts. *Cell Growth & Differ* 4: 483–493.
- Mauviel A, Santra M, Chen YQ, Uitto J, Iozzo RV (1995) Transcriptional regulation of decorin gene expression. Induction by quiescence and repression by tumor necrosis factor- $\alpha$ . *J Biol Chem* 270: 11692–11700.
- Kähäri V-M, Larjava H, Uitto J (1991) Differential regulation of extracellular matrix proteoglycan (PG) gene expression. Transforming growth factor- $\beta$  1 up-regulates biglycan (PGL), and versican (large fibroblast PG) but down-regulates decorin (PGII) mRNA levels in human fibroblasts in culture. *J Biol Chem* 266: 10608–10615.
- Kolettas E, Rosenberger RF (1998) Suppression of decorin expression and partial induction of anchorage-independent growth by the *v-src* oncogene in human fibroblasts. *Eur J Biochem* 254: 266–274.
- Iozzo RV (1988) Proteoglycans and neoplasia. *Cancer Metastasis Rev* 7: 39–50.
- Iozzo RV (1998) Matrix proteoglycans: from molecular design to cellular function. *Annu Rev Biochem* 67: 609–652.
- Iozzo RV (1999) The biology of the small leucine-rich proteoglycans. Functional network of interactive proteins. *J Biol Chem* 274: 18843–18846.
- Keene DR, San Antonio JD, Mayne R, McQuillan DJ, Sarris G, et al. (2000) Decorin binds near the C terminus of type I collagen. *J Biol Chem* 275: 21801–21804.
- Häkkinen L, Strassburger S, Kahari VM, Scott PG, Eichstetter I, et al. (2000) A role for decorin in the structural organization of periodontal ligament. *Lab Invest* 80: 1869–1880.
- Goldoni S, Owens RT, McQuillan DJ, Shriver Z, Sasisekharan R, et al. (2004) Biologically active decorin is a monomer in solution. *J Biol Chem* 279: 6606–6612.
- Schaefer L, Iozzo RV (2008) Biological functions of the small leucine-rich proteoglycans: from genetics to signal transduction. *J Biol Chem* 283: 21305–21309.
- Zhang G, Ezura Y, Chervoneva I, Robinson PS, Beason DP, et al. (2006) Decorin regulates assembly of collagen fibrils and acquisition of biomechanical properties during tendon development. *J Cell Biochem* 98: 1436–1449.
- Robinson PS, Lin TW, Jawad AF, Iozzo RV, Soslowsky LJ (2004) Investigating tendon fascicle structure-function relationship in a transgenic age mouse model using multiple regression models. *Ann Biomed Eng* 32: 924–931.
- Robinson PS, Huang TF, Kazam E, Iozzo RV, Birk DE, et al. (2005) Influence of decorin and biglycan on mechanical properties of multiple tendons in knockout mice. *J Biomechanical Eng* 127: 181–185.
- Iozzo RV, Goldoni S, Berendsen A, Young MF (2011) Small leucine-rich proteoglycans. In: Mecham RP, editors. *Extracellular Matrix: An overview*. Springer. 197–231.
- Kalamajski S, Oldberd Å (2010) The role of small leucine-rich proteoglycans in collagen fibrillogenesis. *Matrix Biol* 29: 248–253.
- Hildebrand A, Romaris M, Rasmussen LM, Heinegård D, Twardzik DR, et al. (1994) Interaction of the small interstitial proteoglycans biglycan, decorin and fibromodulin with transforming growth factor  $\beta$ . *Biochem J* 302: 527–534.
- Ferdous Z, Wei VM, Iozzo RV, Höök M, Grande-Allen KJ (2007) Decorin-transforming growth factor- $\beta$  interaction regulates matrix organization and mechanical characteristics of three-dimensional collagen matrices. *J Biol Chem* 282: 35887–35898.
- Baghy K, Dezső K, László V, Fullár A, Péterfia B, et al. (2011) Ablation of the decorin gene enhances experimental hepatic fibrosis and impairs hepatic healing in mice. *Lab Invest* 91: 439–451.
- Baghy K, Iozzo RV, Kovalszky I (2012) Decorin-TGF $\beta$  axis in hepatic fibrosis and cirrhosis. *J Histochem Cytochem* 60: 262–268.
- Brown EL, Wooten RM, Johnson BJ, Iozzo RV, Smith A, et al. (2001) Resistance to Lyme disease in decorin-deficient mice. *J Clin Invest* 107: 845–852.
- Liang FT, Wang T, Brown EL, Iozzo RV, Fikrig E (2004) Protective niche for *Borrelia burgdorferi* to evade humoral immunity. *Am J Pathol* 165: 977–985.
- Iozzo RV, Schaefer L (2010) Proteoglycans in health and disease: Novel regulatory signaling mechanisms evoked by the small leucine-rich proteoglycans. *FEBS J* 277: 3864–3875.
- Zhu J-X, Goldoni S, Bix G, Owens RA, McQuillan D, et al. (2005) Decorin evokes protracted internalization and degradation of the EGF receptor via caveolar endocytosis. *J Biol Chem* 280: 32468–32479.
- Reed CC, Gauldie J, Iozzo RV (2002) Suppression of tumorigenicity by adenovirus-mediated gene transfer of decorin. *Oncogene* 21: 3688–3695.
- Csordás G, Santra M, Reed CC, Eichstetter I, McQuillan DJ, et al. (2000) Sustained down-regulation of the epidermal growth factor receptor by decorin. A mechanism for controlling tumor growth *in vivo*. *J Biol Chem* 275: 32879–32887.
- Santra M, Eichstetter I, Iozzo RV (2000) An anti-oncogenic role for decorin: downregulation of ErbB2 leads to growth suppression and cytodifferentiation of mammary carcinoma cells. *J Biol Chem* 275: 35153–35161.
- Schönherr E, Sunderkötter C, Iozzo RV, Schaefer L (2005) Decorin, a novel player in the insulin-like growth factor system. *J Biol Chem* 280: 15767–15772.
- Schaefer L, Tsalasra W, Babelova A, Baliova M, Minnerup J, et al. (2007) Decorin-mediated regulation of fibrillin-1 in the kidney involves the insulin-like growth factor-1 receptor and mammalian target of rapamycin. *Am J Pathol* 170: 301–315.
- Merline R, Lazaroski S, Babelova A, Tsalasra-Greul W, Pfeilschifter J, et al. (2009) Decorin deficiency in diabetic mice: aggravation of nephropathy due to overexpression of profibrotic factors, enhanced apoptosis and mononuclear cell infiltration. *J Physiol Pharmacol* 60 (suppl 4): 5–13.
- Iozzo RV, Buraschi S, Genua M, Xu S-Q, Solomides CC, et al. (2011) Decorin antagonizes IGF receptor I (IGF-IR) function by interfering with IGF-IR activity and attenuating downstream signaling. *J Biol Chem* 286: 34712–34721.
- Goldoni S, Humphries A, Nyström A, Sattar S, Owens RT, et al. (2009) Decorin is a novel antagonistic ligand of the Met receptor. *J Cell Biol* 185: 743–754.
- Buraschi S, Pal N, Tyler-Rubinstein N, Owens RT, Neill T, et al. (2010) Decorin antagonizes Met receptor activity and downregulates  $\beta$ -catenin and Myc levels. *J Biol Chem* 285: 42075–42083.
- Schaefer L, Iozzo RV (2012) Small leucine-rich proteoglycans, at the crossroad of cancer growth and inflammation. *Curr Opin Genet Dev* 22: 56–57.
- Seidler DG, Goldoni S, Agnew C, Cardy C, Thakur ML, et al. (2006) Decorin protein core inhibits *in vivo* cancer growth and metabolism by hindering epidermal growth factor receptor function and triggering apoptosis via caspase-3 activation. *J Biol Chem* 281: 26408–26418.
- Patel S, Santra M, McQuillan DJ, Iozzo RV, Thomas AP (1998) Decorin activates the epidermal growth factor receptor and elevates cytosolic  $Ca^{2+}$  in A431 cells. *J Biol Chem* 273: 3121–3124.
- De Luca A, Santra M, Baldi A, Giordano A, Iozzo RV (1996) Decorin-induced growth suppression is associated with upregulation of p21, an inhibitor of cyclin-dependent kinases. *J Biol Chem* 271: 18961–18965.
- Santra M, Mann DM, Mercer EW, Skorski T, Calabretta B, et al. (1997) Ectopic expression of decorin protein core causes a generalized growth suppression in neoplastic cells of various histogenetic origin and requires endogenous p21, an inhibitor of cyclin-dependent kinases. *J Clin Invest* 100: 149–157.
- Moore D, Kohn AD, De Ferrari GV, Kaykas A (2004) Wnt and  $\beta$ -catenin signaling: Diseases and therapies. *Nat Rev Genet* 5: 689–699.
- Albihn A, Johnsen JI, Henriksson MA (2010) MYC in oncogenesis and as a target for cancer therapies. *Adv Cancer Res* 107: 163–224.
- Jung P, Messen A, Mayr D, Hermeking H (2008) AP4 encodes a c-Myc-inducible repressor of p21. *Proc Natl Acad Sci USA* 105: 15046–15051.
- Neill T, Schaefer L, Iozzo RV (2012) Decorin, a guardian from the matrix. *Am J Pathol* 181: 380–387.
- Bi X, Tong C, Dokendorff A, Banroft L, Gallagher L, et al. (2008) Genetic deficiency of decorin causes intestinal tumor formation through disruption of intestinal cell maturation. *Carcinogenesis* 29: 1435–1440.
- Iozzo RV, Chakrani F, Perrotti D, McQuillan DJ, Skorski T, et al. (1999) Cooperative action of germline mutations in decorin and p53 accelerates lymphoma tumorigenesis. *Proc Natl Acad Sci USA* 96: 3092–3097.
- Schönherr E, Sunderkötter C, Schaefer L, Thanos S, Grässel S, et al. (2004) Decorin deficiency leads to impaired angiogenesis in injured mouse cornea. *J Vasc Res* 41: 499–508.
- Järveläinen H, Puolakkainen P, Pakkanen S, Brown EL, Höök M, et al. (2006) A role for decorin in cutaneous wound healing and angiogenesis. *Wound Rep Reg* 14: 443–452.
- Grant DS, Yenisey C, Rose RW, Tootell M, Santra M, et al. (2002) Decorin suppresses tumor cell-mediated angiogenesis. *Oncogene* 21: 4765–4777.
- Neill T, Painter H, Buraschi S, Owens RT, Lisanti MP, et al. (2012) Decorin antagonizes the angiogenic network. Concurrent inhibition of Met, hypoxia

- inducible factor-1 $\alpha$  and vascular endothelial growth factor A and induction of thrombospondin-1 and TIMP3. *J Biol Chem* 287: 5492–5506.
56. Reed CC, Waterhouse A, Kirby S, Kay P, Owens RA, et al. (2005) Decorin prevents metastatic spreading of breast cancer. *Oncogene* 24: 1104–1110.
  57. Goldoni S, Seidler DG, Heath J, Fassan M, Baffa R, et al. (2008) An anti-metastatic role for decorin in breast cancer. *Am J Pathol* 173: 844–855.
  58. Ständer M, Naumann U, Dumitrescu L, Heneka M, Löschmann P, et al. (1998) Decorin gene transfer-mediated suppression of TGF- $\beta$  synthesis abrogates experimental malignant glioma growth in vivo. *Gene Therapy* 5: 1187–1194.
  59. Tralhão JG, Schaefer L, Miccogova M, Evaristo C, Schönherr E, et al. (2003) In vivo selective and distant killing of cancer cells using adenovirus-mediated decorin gene transfer. *FASEB J* 17: 464–466.
  60. Biglari A, Bataille D, Naumann U, Weller M, Zirger J, et al. (2004) Effects of ectopic decorin in modulating intracranial glioma progression *in vivo*, in a rat syngenic model. *Cancer Gene Therapy* 11: 721–732.
  61. Araki K, Wakabayashi H, Shintani K, Morikawa J, Matsumine A, et al. (2009) Decorin suppresses bone metastasis in a breast cancer cell line. *Oncology* 77: 92–99.
  62. Hu Y, Sun H, Owens RT, Wu J, Chen YQ, et al. (2009) Decorin suppresses prostate tumor growth through inhibition of epidermal growth factor and androgen receptor pathways. *Neoplasia* 11: 1042–1053.
  63. Leygue E, Snell L, Dotzlaw H, Troup S, Hiller-Hitchcock T, et al. (2000) Lumican and decorin are differentially expressed in human breast carcinoma. *J Pathol* 192: 313–320.
  64. Troup S, Njue C, Kliever EV, Parisien M, Roskelley C, et al. (2003) Reduced expression of the small leucine-rich proteoglycans, lumican, and decorin is associated with poor outcome in node-negative invasive breast cancer. *Clin Cancer Res* 9: 207–214.
  65. Biaoxue R, Xiguang C, Hua L, Hui M, Shuanying Y, et al. (2011) Decreased expression of decorin and p57 (KIP2) correlates with poor survival and lymphatic metastasis in lung cancer patients. *Int J Biol Markers* 26: 9–21.
  66. Alowami S, Troup S, Al-Haddad S, Kirkpatrick I, Watson PH (2003) Mammographic density is related to stroma and stromal proteoglycan expression. *Breast Cancer Res* 5: R129–R135.
  67. Provenzano PP, Inman DR, Eliceiri KW, Knittel JG, Yan L, et al. (2008) Collagen density promotes mammary tumor initiation and progression. *BMC Medicine* 6: 11.
  68. Maller O, Martinson H, Schedin P (2010) Extracellular matrix composition reveals complex and dynamic stromal-epithelial interactions in the mammary gland. *J Mammary Gland Biol Neoplasia* 15: 301–318.
  69. Howell A, Landberg G, Bergh J (2009) Breast tumor stroma is a prognostic indicator and a target for therapy. *Breast Cancer Res (Suppl 3)*: S16.
  70. Schedin P, O'Brien J, Rudolph M, Stein T, Borges V (2007) Microenvironment of the involuting mammary gland mediates mammary cancer progression. *J Mammary Gland Biol Neoplasia* 12: 71–82.
  71. Iozzo RV, Cohen I (1993) Altered proteoglycan gene expression and the tumor stroma. *Cell Mol Life Sci* 49: 447–455.
  72. Iozzo RV (1995) Tumor stroma as a regulator of neoplastic behavior. Agonistic and antagonistic elements embedded in the same connective tissue. *Lab Invest* 73: 157–160.
  73. Goldoni S, Iozzo RV (2008) Tumor microenvironment: Modulation by decorin and related molecules harboring leucine-rich tandem motifs. *Int J Cancer* 123: 2473–2479.
  74. Huang DW, Sherman BT, Lempicki RA (2009) Systematic and integrative analysis of large gene lists using DAVID bioinformatics resources. *Nat Prot* 4: 44–57.
  75. Chen B, Zhang D, Pollard JW (2003) Progesterone regulation of the mammalian ortholog of methylcitrate dehydratase (*Immune Response Gene 1*) in uterine epithelium during implantation through the protein kinase C pathway. *Mol Endocrinol* 17: 2340–2354.
  76. Lee CGL, Jenkins NA, Gilbert DJ, Copeland NG, O'Brien WE (1995) Cloning and analysis of gene regulation of a novel LPS-inducible cDNA. *Immunogenetics* 41: 263–270.
  77. Degrandi D, Hoffmann R, Beuter-Gunia C, Pfeffer K (2009) The proinflammatory cytokine-induced IRG1 protein associates with mitochondria. *J Interferon Cytokine Res* 29: 55–67.
  78. von Gunten S, Bochner BS (2008) Basic and clinical immunology of Siglecs. *Ann N Y Acad Sci* 1143: 61–68.
  79. Zerrahn J, Schaible UE, Brinkmann V, Gühlich U, Kaufman SHE (2002) The IFN-Inducible Golgi- and endoplasmic reticulum-associated 47-kDa GTPase IIGP is transiently expressed during listeriosis. *J Immunol* 168: 3428–3436.
  80. Sugerman PB, Faber SB, Willis LM, Petrovic A, Murphy GF, et al. (2004) Kinetics of gene expression in murine cutaneous graft-versus-host disease. *Am J Pathol* 164: 2189–2202.
  81. Dharajiya N, Vaidya S, Sinha M, Luxon B, Boldogh I, et al. (2009) Allergen challenge induces I $\kappa$ B dependent GTPases in the lungs as part of Th1 transcriptome response in a murine model of allergic asthma. *PLoS ONE* 4: e8172.
  82. Vesely MD, Kershaw MH, Schreiber RD, Smyth MJ (2011) Natural innate and adaptive immunity to cancer. *Ann Rev Immunol* 29: 235–271.
  83. Marchica CL, Pinelli V, Borges M, Zimmer J, Narayanan V, et al. (2011) A role for decorin in a murine model of allergen-induced asthma. *Am J Physiol Lung Cell Mol Physiol* 300: 863–873.
  84. Seidler DG, Mohamed NA, Bocian C, Stadtmann A, Hermann S, et al. (2011) The role for decorin in delayed-type hypersensitivity. *J Immunol* 187: 6108–6199.
  85. Merline R, Moreth K, Beckmann J, Nastase MV, Zeng-Brouwers J, et al. (2011) Signaling by the matrix proteoglycan decorin controls inflammation and cancer through PDCD4 and microRNA-21. *Sci Signal* 4: ra75.
  86. Liang Q-L, Chen G-Q, Li Z-Y, Wang B-R (2011) Function and histopathology of a cell adhesion molecule TSLC1 in cancer. *Cancer Invest* 29: 107–112.
  87. Heller G, Gerads J, Ziegler B, Newsham I, Filipitis M, et al. (2007) Downregulation of TSLC1 and DAL-1 expression occurs frequently in breast cancer. *Breast Cancer Res Treat* 103: 283–291.
  88. Feng W, Marquez RT, Lu Z, Liu J, Lu KH, et al. (2008) Imprinted tumor suppressor genes *ARHI* and *PEG3* are the most frequently down-regulated in human ovarian cancers by loss of heterozygosity and promoter methylation. *Cancer* 112: 1489–1502.
  89. Maegawa S, Yoshioka H, Itaba N, Kubota N, Nishihara S, et al. (2001) Epigenetic silencing of PEG3 gene expression in human glioma cell lines. *Mol Carcinogen* 31: 1–9.
  90. Rhodes DR, Yu J, Shanker K, Deshpande N, Varambally R, et al. (2004) Large-scale meta-analysis of cancer microarray data identifies common transcriptional profiles of neoplastic transformation and progression. *Proc Natl Acad Sci USA* 101: 9309–9314.
  91. Karnoub AE, Dash AB, Vo AP, Sullivan A, Brooks MW, et al. (2007) Mesenchymal stem cells within tumor stroma promote breast cancer metastasis. *Nature* 449: 557–565.
  92. Richardson AL, Wang ZC, De Nicolo A, Lu X, Brown M, et al. (2006) X chromosomal abnormalities in basal-like human breast cancer. *Cancer Cell* 9: 121–132.
  93. Bissell MJ, Radisky D (2001) Putting tumors in context. *Nat Rev Cancer* 1: 46–54.
  94. Rønnev-Jessen L, Bissell MJ (2009) Breast cancer by proxy: can the microenvironment be both the cause and consequence? *Trends Mol Med* 15: 5–13.
  95. Orimo A, Gupta PB, Sgroi DC, Arenzana-Seisdedos F, Delaunay T, et al. (2005) Stromal fibroblasts present in invasive human breast carcinomas promote tumor growth and angiogenesis through elevated SDF-1/CXCL12 secretion. *Cell* 121: 335–348.
  96. Nikitovic D, Berdiaki K, Chalkiadaki G, Karamanos N, Tzanakakis G (2008) The role of SLRP-Proteoglycans in osteosarcoma pathogenesis. *Connective Tissue Res* 49: 235–238.
  97. Allinen M, Beroukhi R, Cai L, Brennan C, Lahti-Domenici J, et al. (2004) Molecular characterization of the tumor microenvironment in breast cancer. *Cancer Cell* 6: 17–32.
  98. Iozzo RV, Sanderson RD (2011) Proteoglycans in cancer biology, tumour microenvironment and angiogenesis. *J Cell Mol Med* 15: 1013–1031.
  99. Finak G, Bertos N, Pepin F, Sadekova S, Souleimanova M, et al. (2008) Stromal gene expression predicts clinical outcome in breast cancer. *Nat Med* 14: 518–527.
  100. Ma X-J, Salunga R, Tuggle JT, Gaudet J, Enright E, et al. (2003) Gene expression profiles of human breast cancer progression. *Proc Natl Acad Sci USA* 100: 5974–5979.
  101. Ma X-J, Dahiya S, Richardson E, Erlander M, Sgroi DC (2009) Gene expression profiling of the tumor microenvironment during breast cancer progression. *Breast Cancer Res* 11: R7.
  102. Jiang X, Yu Y, Yang HW, Agar NYR, Frado L, et al. (2010) The imprinted gene *PEG3* inhibits Wnt signaling and regulates glioma growth. *J Biol Chem* 285: 8472–8480.
  103. Deng Y, Wu X (2000) Peg3/Pw1 promotes p53-mediated apoptosis by inducing Bax translocation from cytosol to mitochondria. *Proc Natl Acad Sci USA* 97: 12050–12055.
  104. Kearns AE, Donohue MM, Sanyal B, Demay MB (2001) Cloning and characterization of a novel protein kinase that impairs osteoblast differentiation *in vitro*. *J Biol Chem* 276: 42213–42218.
  105. Tamimi Y, Lines M, Coca-Prados M, Walter MA (2004) Identification of target genes regulated by *FOXO1* using nickel agarose-based chromatin enrichment. *Invest Ophthalmol Vis Sci* 45: 3904–3913.
  106. Liu H-P, Lin Y-J, Lin W-YWL, Sheu JJ-C, Lin H-J, et al. (2009) A novel genetic variant of *BMP2k* contributes to high myopia. *J Clin Lab Anal* 23: 362–367.
  107. Gao G, Guo X, Goff SP (2002) Inhibition of retroviral RNA production by ZAP, a CCH-type zinc finger protein. *Science* 297: 1703–1706.
  108. Zhu Y, Chen G, Lv F, Wang X, Ji X, et al. (2011) Zinc-finger antiviral protein inhibits HIV-1 infection by selectively targeting multiply spliced viral mRNAs for degradation. *Proc Natl Acad Sci USA* 108: 15834–15839.
  109. Sodik NM, Swigart LB, Karnezis AN, Hanahan D, Evan GI, et al. (2011) Endogenous Myc maintains the tumor microenvironment. *Genes Dev* 25: 907–916.
  110. Salnikow AV, Roswall P, Sundberg C, Gardner H, Heldin N-E, et al. (2005) Inhibition of TGF- $\beta$  modulates macrophages and vessel maturation in parallel to a lowering of interstitial fluid pressure in experimental carcinoma. *Lab Invest* 85: 512–521.
  111. Chiavarina B, Whitaker-Menezes D, Migneco G, Martinez-Outschoorn UE, Pavlides S, et al. (2010) HIF1- $\alpha$  functions as a tumor promoter in cancer



- associated fibroblasts, and as a tumor suppressor in breast cancer cells. Autophagy drives compartment-specific oncogenesis. *Cell Cycle* 9: 3534–3551.
112. Ramamurthy P, Hocking AM, McQuillan DJ (1996) Recombinant decorin glycoforms. Purification and structure. *J Biol Chem* 271: 19578–19584.
113. Cohen IR, Murdoch AD, Naso MF, Marchetti D, Berd D, et al. (1994) Abnormal expression of perlecan proteoglycan in metastatic melanomas. *Cancer Res* 54: 5771–5774.
114. Ryyänen M, Ryyänen J, Solberg S, Iozzo RV, Knowlton RG, et al. (1992) Genetic linkage of Type VII collagen (COL7A1) to dominant dystrophic epidermolysis bullosa in families with abnormal anchoring fibrils. *J Clin Invest* 89: 974–980.